



#### OPEN ACCESS

##### EDITED BY

Robert Klinger,  
Belize Foundation for Research and  
Environmental Education, Belize

##### REVIEWED BY

Ruei-Yuan Wang,  
Guangdong University of Petrochemical  
Technology, China  
Xiaoyu Liang,  
University of California, Davis,  
United States

##### \*CORRESPONDENCE

Zhijia Gu  
✉ [guzhijia@xynu.edu.cn](mailto:guzhijia@xynu.edu.cn)

RECEIVED 09 December 2025

REVISED 09 February 2026

ACCEPTED 09 February 2026

PUBLISHED 02 March 2026

##### CITATION

Gu Z, Xu G, Feng L, Li Y, Ji K and  
Reheman M (2026) Spatiotemporal  
dynamics and driving factors of drought  
in the Yellow River Basin (Henan  
section): insights from TVDI analysis.  
*Front. Ecol. Evol.* 14:1763944.  
doi: 10.3389/fevo.2026.1763944

##### COPYRIGHT

© 2026 Gu, Xu, Feng, Li, Ji and Reheman.  
This is an open-access article distributed  
under the terms of the [Creative  
Commons Attribution License \(CC BY\)](https://creativecommons.org/licenses/by/4.0/).  
The use, distribution or reproduction in  
other forums is permitted, provided the  
original author(s) and the copyright  
owner(s) are credited and that the  
original publication in this journal is  
cited, in accordance with accepted  
academic practice. No use, distribution  
or reproduction is permitted which does  
not comply with these terms.

# Spatiotemporal dynamics and driving factors of drought in the Yellow River Basin (Henan section): insights from TVDI analysis

Zhijia Gu<sup>1,2\*</sup>, Gaohan Xu<sup>1,2</sup>, Liu Feng<sup>3</sup>, Yishan Li<sup>4</sup>, Keke Ji<sup>1,2</sup>  
and Maidinamu Reheman<sup>1,2</sup>

<sup>1</sup>School of Geographical Sciences, Xinyang Normal University, Xinyang, China, <sup>2</sup>North–South Transitional Zone Typical Vegetation Phenology Observation and Research Station of Henan Province, Xinyang, China, <sup>3</sup>Business School, Xinyang Vocational and Technical College, Xinyang, China, <sup>4</sup>Zhengzhou Lishui Foreign Language School, Zhengzhou, China

**Introduction:** Located in central China, the Yellow River Basin (Henan section) is a vital grain-producing region with extensive farmland. Its strategic central location also means its economic development is crucial for the stable growth of both Henan Province and the national economy. Nevertheless, persistent drought has long presented significant challenges to the region's agriculture, ecology, and economic development.

**Methods:** Based on TVDI (Temperature Vegetation Dryness Index) data from 2003 to 2022, this study investigated historical drought dynamics through Theil–Sen Median and Mann–Kendall trend analyses. Future drought tendencies were assessed using R/S analysis. Spatiotemporal influencing factors were further examined using Geographic Detector.

**Results:** Research results indicated that most areas of the region were experiencing drought conditions. From 2003 to 2022, drought intensified in the northeastern counties of Yuanyang, Fengqiu, Changyuan, Puyang, Fanxian, and Taiqian within the Yellow River Basin (Henan section), while drought conditions eased in the southwestern counties of Lingbao, Lushi, Luoning, Shanzhou District, and Jiyuan. Future trends in drought variation indicated that the southwestern part of the region showed potential for improvement in drought conditions, while drought conditions in the western areas were likely to worsen. The primary factors influencing the spatiotemporal variation of drought in this region were evapotranspiration, temperature, and rainfall.

**Discussion:** This study aimed to provide an in-depth analysis of the drought situation in the Yellow River Basin (Henan section), offering a reference to assist stakeholders in implementing timely drought mitigation measures, thereby reducing the impact of drought on agricultural production and the ecological environment.

##### KEYWORDS

drought, geographic detector, Hurst exponent, TVDI (Temperature Vegetation Dryness Index), Yellow River Basin (Henan section)

# 1 Introduction

Drought, a prolonged period of exceptionally dry weather resulting in a serious hydrological imbalance, ranks among the most widespread and impactful natural disasters globally (Field et al., 2012). It triggers a cascade of severe environmental consequences, including soil degradation, desertification, vegetation die-off, and an increased frequency of sandstorms and wildfires (Guo et al., 2017; Wang et al., 2023), thereby posing significant threats to ecosystems, agricultural productivity, and socioeconomic stability (Abbas and Ali, 2024; Wu et al., 2025; Zhu et al., 2025). Agricultural drought, a category of drought, results from an imbalance between crop water demand and available soil moisture, directly translating meteorological water shortages into agricultural losses (Guo et al., 2020; Chen et al., 2021; Alazba et al., 2025). It arises from an imbalance between crop water demand and soil water supply and is considered one of the direct consequences of meteorological drought (Liu and Li, 2024). Under global climatic and environmental change, China's status as a major agricultural nation renders its food systems especially susceptible to drought stress (Wang et al., 2019). Such conditions critically—and often decisively—limit rain-fed crop productivity. This is especially evident in the North China Plain, where a trend of declining rainfall has heightened the frequency of drought events, which often persist across consecutive seasons or even years (Wen et al., 2023).

Effective monitoring is fundamental to drought mitigation. While traditional ground-based methods for obtaining soil moisture data face significant challenges, their sparse observational networks limit reliable large-scale spatial assessment and forecasting (Almouctar et al., 2024). The advent of remote sensing has revolutionized this field by enabling synoptic, repetitive earth observation. Consequently, numerous remote sensing-based drought indices have been developed, such as the Vegetation Condition Index (VCI), the Soil Moisture Agricultural Drought Index (SMADI), and the Temperature Vegetation Dryness Index (TVDI). Among these, the TVDI, derived from the negative correlation between land surface temperature (LST) and vegetation indices (e.g., NDVI, EVI) in a feature space, offers distinct advantages for agricultural drought monitoring. It physically reflects soil moisture status, is particularly sensitive in vegetated and cropland areas, and leverages widely available MODIS data, ensuring operational feasibility and comparability across studies (Bai et al., 2017; Sandholt et al., 2002). This makes TVDI a robust tool for analyzing the spatiotemporal dynamics of drought. Therefore, it has been widely used in regional drought dynamic monitoring (Zormand et al., 2017; Chen et al., 2018; Ali et al., 2019; Alazba et al., 2025; Zou et al., 2025). It is now established as a principal indicator for assessing agricultural drought severity in China (Wan et al., 2021; Huang et al., 2025).

The Yellow River Basin is a vital ecological security barrier and a major socioeconomic corridor in China. Ecological conservation and high-quality development of the basin has been designated as major national strategies. As a vital segment of the Yellow River Basin, the Henan section serves as a significant grain production

base in China and encompasses multiple national key ecological function zones. Its role in promoting the holistic development of the entire Yellow River Basin is therefore indispensable (Yan et al., 2022). This region boasts a strategic geographical location, serving as a vital transportation nexus connecting North China, Central China, and the Southwest (Liu et al., 2023). It is also a key area under China's Western Development Strategy, playing a significant role in supporting the stable economic growth of both Henan Province and the nation as a whole part. Drought has long been a major constraint on production, livelihoods, and economic development in this region (Zhao et al., 2022; Li Y. et al., 2024). Despite the application of remote sensing for drought monitoring in broader contexts, a distinct knowledge gap persists regarding the long-term spatiotemporal patterns and the specific drivers of drought within the Yellow River Basin (Henan section). Existing studies often focus on single factors or short periods, lacking a comprehensive, long-term analysis that integrates climatic and anthropogenic drivers—such as precipitation, temperature, evapotranspiration, and human activity indicators—to explain drought dynamics in this ecologically and economically sensitive transition zone. To address this research gap, based on TVDI from 2003 to 2022, this study investigates the spatiotemporal dynamics and driving factors of drought in the Yellow River Basin (Henan section). Therefore, this study aimed to (1) characterize the spatiotemporal evolution of drought through Theil–Sen Median, Mann–Kendall trend analysis and R/S analysis; and (2) quantify the relative influence and interaction of key natural and anthropogenic driving factors using the geodetector. Our findings are expected to contribute to accurate drought monitoring and evaluation, provide a scientific basis for predicting future drought trends, and support the timely implementation of drought mitigation measures.

## 2 Materials and methods

### 2.1 Study area

The Yellow River Basin (Henan section) is located in the central part of China. Its geographical coordinates range from 33°31' N to 36°22' N, and from 110°21' E to 116°05' E. The main course of the river spans 711 km, the terrain tends to be higher in the southwest and lower in the northeast, with the lowest elevation of 35 m. The plain area in the eastern part of the study area belongs to the Huang Huai Hai alluvium plain in the eastern part of Henan Province, which is flat, rich in land resources and has a long history of farming (Figure 1). Henan section accounts for 5.1% of the total drainage area of the Yellow River Basin (Fan, 2016). It is situated in the middle and lower reaches of the Yellow River, spanning the second and third terrain steps of China. The vegetation in the Henan section of the Yellow River Basin is dominated by cultivated crops, with farmland accounting for 76.51% of the total study area, followed by forestland, which makes up 13.79% (Cui et al., 2025). The increase in urban land use and the decrease in cultivated land in the future will both lead to an increase in TVDI, resulting in a higher degree of drought in urban

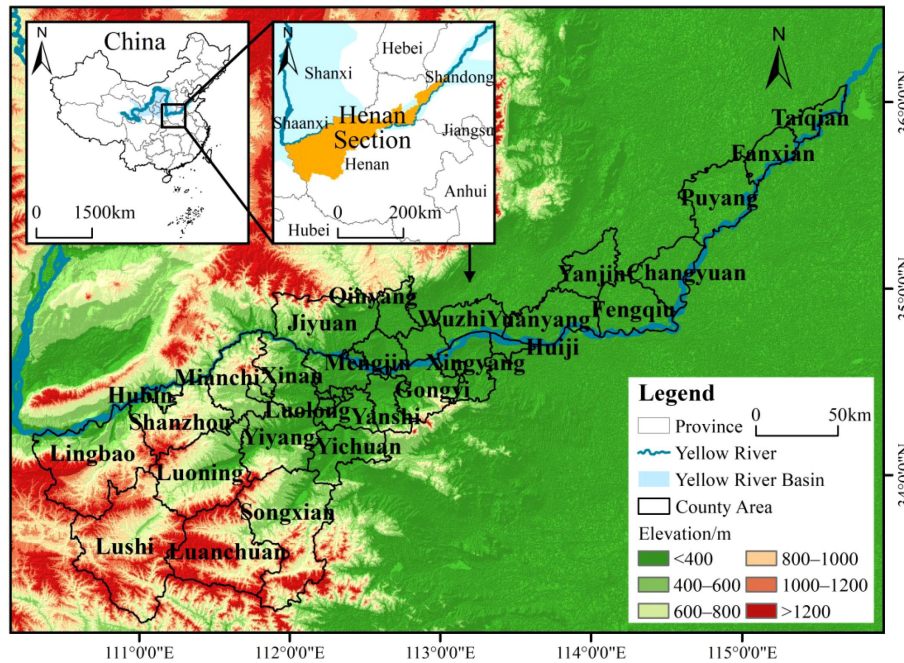


FIGURE 1 The location of the study area.

areas. The region lies in a transitional zone between the temperate monsoon climate and the subtropical monsoon climate, characterized by four distinct seasons and precipitation concentrated mainly in the summer. The average annual temperature showed a significant increasing trend, with the fastest rates of increase observed in spring and autumn, while precipitation showed significant interannual variability (Yao et al., 2024). The study area is trending toward increased aridity. However, constrained by its natural geography and historical development, the region is characterized by an inadequate total water supply, uneven spatiotemporal distribution, and poor water quality. The region faces significant challenges in water resource management. Water use efficiency remains relatively low, with an agricultural irrigation efficiency coefficient of only 0.55—well below advanced international standards. Meanwhile, the exploitation rate of water resources has reached 80%, far exceeding the internationally recognized warning threshold of 40% for river water resource development. As the population grows and the economy expands, the imbalance between water supply and demand is becoming increasingly acute. Water scarcity has emerged as a major constraint to the region’s high-quality development.

## 2.2 Data sources and preprocessing

The TVDI data in this paper is sourced from the 2003–2022 annual 1 km resolution dataset of TCI, VCI, VHI, and TVDI for the Yellow River Basin (https://doi.org/10.57760/sciedb.09116) (Sha et al., 2024). The precipitation, temperature, and potential evapotranspiration data were obtained from the National Tibetan Plateau Data Center (https://data.tpcd.ac.cn), with a spatial resolution of 1 km. The Digital Elevation Model (DEM) data with a spatial resolution of 30m of the study area was obtained from the

Geospatial Data Cloud (https://www.gscloud.cn). Nighttime light data with a spatial resolution of 0.0042° were acquired from the Data Center for Resources and Environmental Sciences, Chinese Academy of Sciences (https://www.resdc.cn). The 1 km resolution spatial distribution data of population density were obtained from the LandScan dataset (https://landscan.ornl.gov). All data were converted to Tiff format, the projection was converted to WGS-1984 coordinate system, and the spatial resolution was uniformly resampled to 1 km.

## 2.3 Methods

The structural flowchart of the study was shown in Figure 2. The research methods employed in this study will be comprehensively elaborated in the current section.

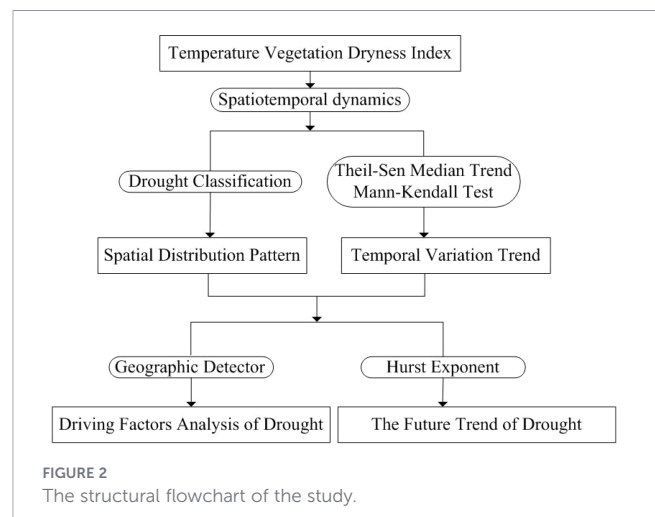


FIGURE 2 The structural flowchart of the study.

### 2.3.1 TVDI model

This study applied the TVDI model (Equation 1) to inversion processing of remote sensing data. Based on the triangular distribution pattern observed in the NDVI–LST scatter plot, Sandholt et al. (2002) revealed a significant negative correlation between LST and NDVI. As vegetation coverage increases, transpiration effects reduce surface temperatures, which led to the proposal of the TVDI. TVDI is calculated from vegetation indices and land surface temperature using the formula as follows:

$$TVDI = \frac{t_s - t_{smin}}{t_{smax} - t_{smin}} \tag{1}$$

where  $t_s$  is surface temperature value (°C).  $t_{smin}$  is the minimum surface temperature value of all grid values under the same vegetation cover condition.  $t_{smax}$  is the maximum surface temperature value of all grid values under the same vegetation cover condition.

The TVDI ranges from 0 to 1, serves as an indicator of surface soil moisture status. An increase in TVDI corresponds to decreased soil moisture and intensified drought severity, while a decrease indicates increased moisture and wetter conditions. Consequently, values closer to 1 represent more extreme drought, and values approaching 0 reflect higher moisture levels. In accordance with prior research and the prevailing conditions of the study area (Su et al., 2024), TVDI was categorized into five grades, as presented in Table 1.

### 2.3.2 Theil–Sen Median trend analysis and Mann–Kendall significance test

This study first employed the Theil–Sen Median trend analysis method to analyze the multi-year TVDI within the region, clarifying its changing trends. Subsequently, the Mann–Kendall significance test was applied to determine the statistical significance of these trends. The combination of these two methods (Guo et al., 2018; Wang et al., 2023) provides a more robust identification of changes in drought severity for the study area.

The Theil–Sen Median trend analysis is a non-parametric statistical method used to estimate data trends. This method is relatively insensitive to outliers in the data, offers strong robustness, and can more accurately reflect the overall trend. Furthermore, as long as the data exhibits a general trend, the Sen’s slope estimate can provide a reasonable assessment of that trend. It is calculated as follows:

Given a set of points  $(x_i, y_i)$ , where  $i = 1, 2, 3, \dots, n$ . compute the slope ( $s_{ij}$ ) for all possible pairwise combinations of points  $(x_i, y_i)$  and  $(x_j, y_j)$  ( $i \neq j$ ) (Equation 2).

$$s_{ij} = \frac{y_j - y_i}{x_j - x_i} \tag{2}$$

Arrange all the slopes( $s_{ij}$ ) in ascending order, and take the median as the Sen’s slope estimate  $\beta$ . After obtaining the result  $\beta$ , if  $\beta > 0$ , it indicates an increasing trend in the data from  $x_i$  to  $x_j$ ; conversely, if  $\beta < 0$ , it suggests a decreasing trend.

Mann–Kendall test was used to test the significance of the change trend (Mann, 1945; Kendall, 1975). The Mann–Kendall significance test is primarily used to determine whether a long-term time series exhibits a statistically significant monotonic trend (upward or downward). The calculation procedure is as follows (Equations 3–9):

It is assumed that the time series possesses no statistically significant monotonic trend, and that the data are structured in a random order. Given a time series  $x_1, x_2, \dots, x_n$ ,  $n = 1, 2, 3, \dots, n$ . Compute the value of S:

$$S = \sum_{i=1}^{n-1} S_i \tag{3}$$

$$S_i = \sum_{j=i+1}^n \text{sgn}(x_j - x_i), i = 1, 2, \dots, n - 1 \tag{4}$$

$$\text{sgn}(x_j - x_i) = \begin{cases} +1, & x_j > x_i \\ 0, & x_j = x_i \\ -1, & x_j < x_i \end{cases} \tag{5}$$

Calculate the expected value  $E(S)$  and variance  $Var(S)$  of S. When the sample size  $n$  is sufficiently large ( $n > 10$ ), the statistic S approximately follows a normal distribution. Its mean is  $E(s) = 0$ . A two-tailed trend test is employed to determine the statistical significance of the change trend in the data series. Compute the test statistic Z:

$$Z = \begin{cases} \frac{S-1}{\sqrt{var(S)}}, & S > 0 \\ 0, & S = 0 \\ \frac{S+1}{\sqrt{var(S)}}, & S < 0 \end{cases} \tag{6}$$

$$S = \sum_{i=1}^{n-1} \sum_{j=i+1}^n \text{sign}(TVDI_j - TVDI_i) \tag{7}$$

$$var(S) = \frac{n(n+1)(2n+5)}{18} \tag{8}$$

$$\text{sign}(TVDI_j - TVDI_i) = \begin{cases} 1, & TVDI_j - TVDI_i > 0 \\ 0, & TVDI_j - TVDI_i = 0 \\ -1, & TVDI_j - TVDI_i < 0 \end{cases} \tag{9}$$

In the formula,  $n$  represents the length of the data, and  $TVDI_i$  and  $TVDI_j$  are the TVDI values in the TVDI time series

TABLE 1 TVDI–based drought classification.

Grade	Types	TVDI
1	Normal	0 < TVDI < 0.46
2	Mild drought	0.46 ≤ TVDI < 0.57
3	Moderate drought	0.57 ≤ TVDI < 0.76
4	Severe drought	0.76 ≤ TVDI < 0.86
5	Extreme drought	0.86 ≤ TVDI < 1.0

corresponding to years  $i$  and  $j$ , respectively. In this study,  $|Z|$  greater than 2.58 indicates an extremely significant change trend.  $|Z|$  between 1.96 and 2.58 is considered significant change trend.  $|Z|$  between 1.65 and 1.96 is classified as slight significant. and  $|Z|$  less than 1.65 suggests no statistically significant trend. The specific criteria for determining the significance of trends are presented in Table 2.

### 2.3.3 Hurst exponent

Originally developed by British hydrologist Hurst (1951) and later refined by Mandelbrot and Wallis (1969), the Hurst exponent method assesses the sustainability of time series data. This critical metric, derived from Rescaled Range (R/S) analysis, quantifies long-term memory and persistence. By leveraging historical patterns, it enables predictions of future trends. The core principle is outlined below (Equations 10–13).

Establish a time series of TVDI,  $\overline{TVDI}(\tau)$ ,  $\tau = 1, 2, \dots, n$ . Define the mean sequence of the time series:

$$\overline{TVDI}(\tau) = \frac{1}{\tau} \sum_{t=1}^{\tau} TVDI(t) \quad \tau = 1, 2, \dots, n \quad (10)$$

Calculate the accumulated deviation:

$$X(\tau) = \sum_{t=1}^{\tau} (TVDI(t) - \overline{TVDI}(\tau)) \quad \tau = 1, 2, \dots, n \quad (11)$$

Establish a range sequence:

$$R(\tau) = \max_{(1 \leq t \leq \tau)} TVDI(t) - \min_{(1 \leq t \leq \tau)} TVDI(t) \quad \tau = 1, 2, \dots, n \quad (12)$$

Establish a standard deviation sequence:

$$S(\tau) = \left[ \frac{1}{\tau} \sum_{t=1}^{\tau} (TVDI(t) - \overline{TVDI}(\tau))^2 \right]^{\frac{1}{2}} \quad \tau = 1, 2, \dots, n \quad (13)$$

If present  $R/S \propto \tau^H$ , this indicates the existence of the Hurst phenomenon in the TVDI time series. The Hurst exponent (denoted as  $H$ ) is quantitatively determined through least squares fitting.

The Hurst exponent ( $H$ ) ranges from 0 to 1, with three distinct scenarios (Bhattacharya et al., 1983).  $H > 0.5$ : Indicates persistent behavior in the time series. The  $H$  value approaching 1 indicates strong persistence, meaning the future trend is likely to continue the past direction. The  $H$  value of 0.5 signifies a random, uncorrelated series without a discernible trend. Conversely, the  $H$  value below 0.5 demonstrates anti-persistence, suggesting the future trend is likely to reverse the past direction. To better understand the persistence of future TVDI change trends in the Yellow River Basin (Henan section), this study calculated the Hurst index of TVDI on a pixel-by-pixel basis. By integrating these results with the Sen's trend results that passed the significance test, the relationship between the future direction of drought changes and the past trend in the Yellow River Basin (Henan section) was determined.

### 2.3.4 Geographic detector

The geographic detector can analyze the influence of different independent variables on the spatial distribution pattern of specific dependent variables (Wang and Xu, 2017). It contains the following four detectors: factor detection, interaction detection, risk detection, and ecological detection.

1) Factor detector.

A factor detector could determine the effect of detecting the spatial heterogeneity of vegetation change. The spatial heterogeneity of  $X$  to  $Y$  could be expressed as  $q \times 100\%$ , and the greater the number, the greater the influence of the detection factors on vegetation change (Deng et al., 2022), which is as follows (Equation 14):

$$q = 1 - \frac{\sum_{h=1}^L N_h \sigma_h^2}{N \sigma^2} \quad (14)$$

where  $q$  represents the influence of the factor on the dependent variable.  $h$  denotes the stratification of influencing factors.  $L$  indicates the number of sub-regions.  $N$  and  $N_h$  are the sample sizes of the entire region and the  $h$ -th ( $h=1, \dots, L$ ) sub-region of the variable, respectively.  $\sigma^{2h}$  and  $\sigma^2$  are represent the variances of the influencing factors for the entire region,  $h$ -th sub-region, respectively. A large  $q$  indicates a high explanation of the spatial heterogeneity (Chen et al., 2020).

2) Interaction detector.

Interaction detector was used to assess interaction between two factors. The  $q$  values of individual factors  $q(X1)$  and  $q(X2)$  were first calculated separately, and the value of two-factor interaction  $q(X1 \cap X2)$  was calculated.  $\min(q(X1), q(X2))$  represents the minimum value between  $X1$  and  $X2$ .  $\max(q(X1), q(X2))$  represents the maximum value between  $X1$  and  $X2$ . The sum of  $X1$  and  $X2$  is  $q(X1) + q(X2)$ . The interaction between  $X1$  and  $X2$  is  $q(X1 \cap X2)$ . The results are defined by comparing the  $q$  value of individual factor and two-factor interaction as shown in Table 3.

Vegetation coverage, vegetation evapotranspiration, precipitation, temperature, elevation, slope gradient, population density, and nighttime light were selected. This study employed the factor detector and interaction detector within the Geodetector to analyze the influences of precipitation (PRE), temperature (TMP),

TABLE 2 Trend analysis and significance evaluation.

$\beta$	Types	Variation trend
$\beta > 0$	$2.58 \leq Z$	Extremely significant increase
	$1.96 \leq Z < 2.58$	Significant increase
	$1.65 \leq Z < 1.96$	Slight significant increase
	$0 \leq Z < 1.65$	Not significant increase
$\beta = 0$	$ Z  < 1.65$	No change
$\beta < 0$	$-1.65 < Z \leq 0$	Not significant decrease
	$-1.96 < Z \leq -1.65$	Slight significant decrease
	$-2.58 < Z \leq -1.96$	Significant decrease
	$Z \leq -2.58$	Extremely significant decrease

TABLE 3 Categories of factor interactions.

Foundation	Interaction
$q(X1 \cap X2) < \text{Min}(q(X1), q(X2))$	Nonlinear weakening: The interaction of two variables nonlinearly weakens the impacts of single variables.
$\text{Min}(q(X1), q(X2)) \leq q(X1 \cap X2) \leq \text{Max}(q(X1), q(X2))$	Single factor nonlinear weakening: The impacts of individual variables are weakened by the interaction, resulting in a single factor nonlinear weakening effect.
$q(X1 \cap X2) > \text{Max}(q(X1), q(X2))$	Double factor enhancement: The impact of single variables is enhanced by the interaction, resulting in a double factor enhancement effect.
$q(X1 \cap X2) = q(X1) + q(X2)$	Independence: The impacts of variables are assumed to be independent.
$q(X1 \cap X2) > q(X1) + q(X2)$	Nonlinear enhancement: The effects of variables are enhanced in a non-linear manner.

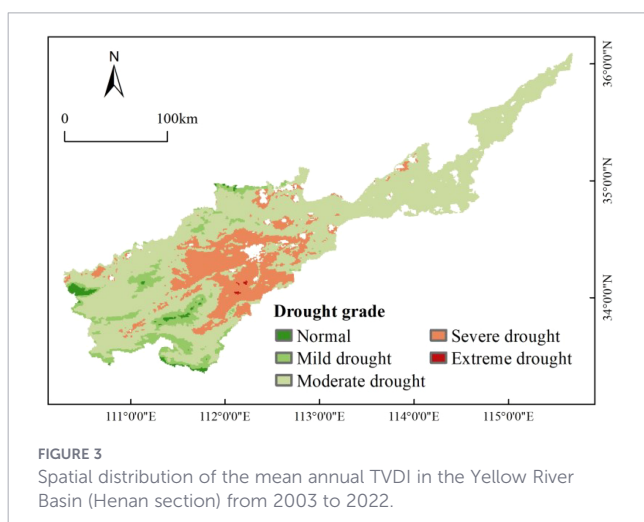
evapotranspiration (ET), slope, GDP, nighttime light (NPP-VIIRS), elevation (ELE), and population density (POP) on drought conditions (as represented by TVDI) in the Yellow River Basin (Henan section). The factor detector was used to identify their explanatory power.

### 3 Results

#### 3.1 Spatiotemporal distribution characteristics of drought

##### 3.1.1 Spatial distribution characteristics of drought

Based on the spatial distribution of TVDI, the majority of the study area was experiencing drought conditions. Of the total area, 70.63% was classified as being in a state of moderate drought, followed by severe drought, which accounted for 19.28% (Figure 3). Areas under normal conditions accounted for only 1.14% of the total study area. Mild drought areas were distributed along the periphery of these normal zones. Severe drought areas were concentrated in the northeastern part of Luoyang City, encompassing Yiyang County, Yichuan County, Song County, Mengjin County, the southeastern



part of Xin'an County, and Luolong District. Normal conditions were found only in small southwestern areas of Lingbao City in Sanmenxia City, marginal areas of Luanchuan County in Luoyang City, and the northern fringe of Jiyuan City.

##### 3.1.2 Temporal variation trend of drought

As illustrated in Figure 4a, the TVDI trend from 2003 to 2022 exhibited pronounced spatial heterogeneity across the Yellow River Basin (Henan section). The entire region showed a general increasing gradient from southwest to northeast, which indicated a progressive intensification of drought conditions in that direction. Drought severity alleviated in the southwestern region, reflecting an improvement in conditions. In contrast, the northeastern region experienced a notable intensification of drought, and this worsening trend became increasingly evident. Through statistical analysis of the change trends across categories (Figure 4b), the areal proportions corresponding to each grade level were derived. A decrease trend (including extremely significant decrease, significant decrease, slight significant decrease, and not significant decrease) in TVDI accounted for 41.17% of the study area, while a significant increase was observed in 15.82% of the region. Significant decrease trend of TVDI was primarily located in southern Lingbao, Lushi, Shanzhou, and northern Mianchi, Jiyuan City, Luoning County and northern Xin'an County in Luoyang City, with small portions of southern Yiyang County, western Luanchuan County, southern Song County, and the border area between Yanshi and Yichuan, have shown a gradual improvement in drought conditions over the study period. The proportion of the area showing an increasing trend in TVDI was 56.7%. The central and northeastern parts of the study area demonstrated a significant increasing trend of TVDI. It is indicated that the drought in these areas was becoming more severe. A considerable portion (23.58%) of the study area was classified as experiencing an extremely significant increase.

##### 3.1.3 Prediction of future drought trends based on R/S analysis

The average Hurst exponent in the study area is 0.46, which may signal the end or reversal of drought conditions in the region. Hurst exponent values of less than 0.5 were observed in approximately 70% of the study area (Figure 5a). This implies that for the majority of the study area, the drought situation is expected to be the opposite of the past.

The increase (weak anti-persistence) area accounts for the largest proportion of the area at 29.04%, primarily distributed in the central and northeastern parts of the study area. The decrease (weak anti-persistence) area occupies the second-largest proportion of the area at 26.55%, mainly located in the western part of the study area (Figure 5b). Drought conditions in these regions are expected to further alleviate. The increase (weak persistence and strong persistence) areas are mainly distributed in the northeastern part of the study area, accounting for 17.43% and 2.29% of the total area, respectively. Drought conditions in these regions are likely to further intensify in the future, primarily located in Wuzhi County and the southern part of Qinyang City in Jiaozuo City, the southwestern part of Yuanyang County in Xinxiang City,

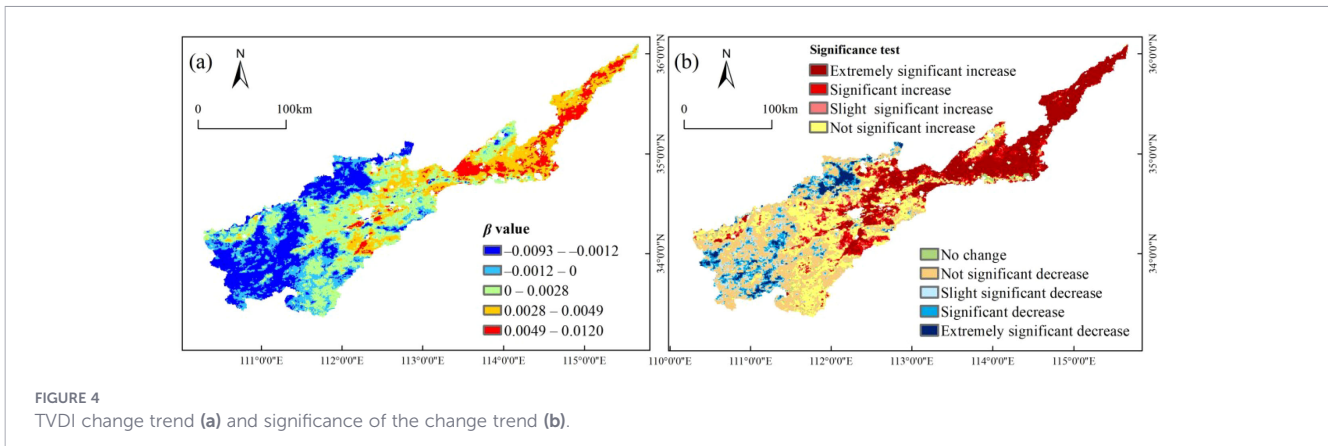


FIGURE 4 TVDI change trend (a) and significance of the change trend (b).

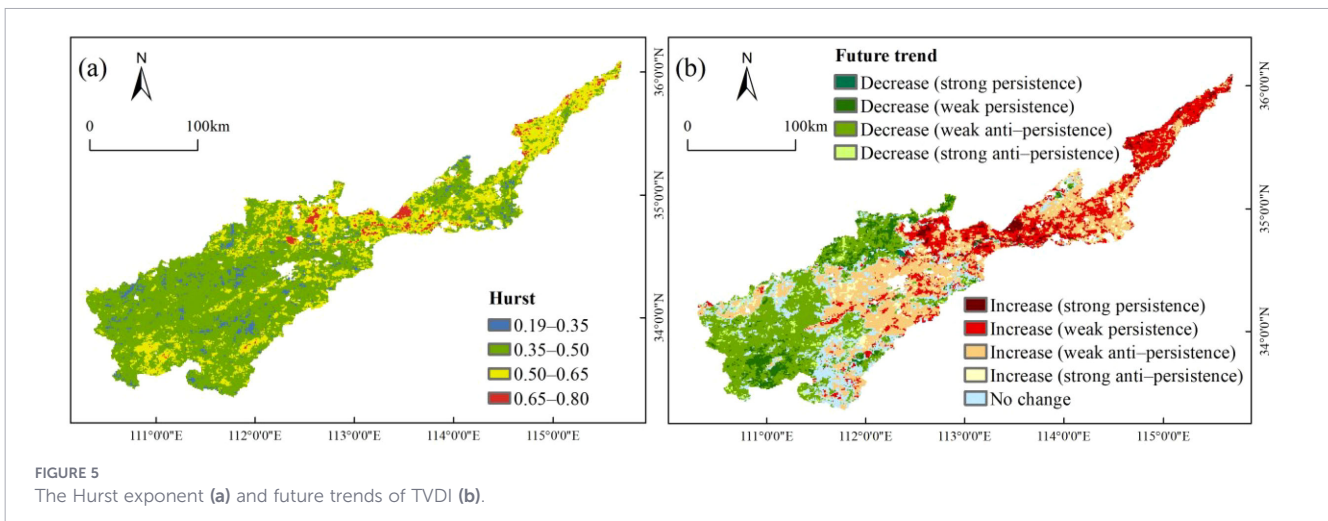


FIGURE 5 The Hurst exponent (a) and future trends of TVDI (b).

as well as Puyang County, Fan County, and Taiqian County. The areas classified as “decrease (strong persistence)” and “decrease (weak persistence)” account for relatively small proportions, primarily distributed in Lushi County of Sanmenxia City and certain parts of Jiyuan City. Drought conditions in these regions are expected to gradually improve in the future, and this alleviation trend is not temporary but demonstrates a certain degree of stability and long-term persistence.

### 3.2 Driving factors analysis of drought

#### 3.2.1 Analysis of single factor influence

To investigate the driving mechanisms behind changes in drought levels in the Yellow River Basin (Henan section), this study selected factors from three aspects: human activity factors, topographic factors, and climatic factors for each year. Geodetector

was used to analyze the explanatory power of each factor on the drought severity in the Yellow River Basin (Henan section). The single-factor detection results showed that the  $p$ -values for evapotranspiration and temperature were less than 0.01, indicating that ET, TMP and PRE have a highly significant impact on the spatial distribution of drought in the Yellow River Basin (Henan section). From the  $q$ -values in the Table 4, it can be observed that the differences in the explanatory power of the driving factors for drought in the Yellow River Basin (Henan section) are relatively small, though still notable. The analysis of  $q$ -values revealed that ET held the greatest explanatory power for TVDI ( $q = 0.90$ ), closely followed by TMP ( $q = 0.89$ ) and PRE ( $q = 0.85$ ). It indicates that ET, TMP and PRE are the dominant factors influencing TVDI in the Yellow River Basin (Henan section). NPP-VIIRS has the lowest explanatory power for TVDI. Overall, changes in drought severity in the Yellow River Basin (Henan section) are primarily influenced by ET, TMP and PRE. Compared

TABLE 4 Single-factor detector analysis.

Statistical index	GDP	SLOPE	ET	TMP	POP	NPP-VIIRS	ELE	PRE
$q$ value	0.13	0.24	0.90	0.89	0.23	0.10	0.17	0.85
$p$ value	0.27	0.16	0.00	0.00	0.17	0.58	0.17	0.00

to topographic factors and human activities, climatic factors exhibit stronger explanatory power for environmental changes.

### 3.2.2 Interaction analysis of driving factors

The Geodetector was employed in this section to analyze the interactions among driving factors on drought (Figure 6). The interaction between TMP and POP demonstrated the strongest detection effect, reaching 0.99, which was higher than that of other combinations, followed by the interactions between ET and POP (0.98) and between PRE and POP (0.98). Although GDP, SLOPE, NPP-VIIRS and ELE were not significant in the single-factor detection, their explanatory power for the dependent variable increased when interacting with other factors. This indicates that the individual effects of these factors are not sufficient to influence the drought conditions in the study area. However, the geographical environment is a whole and the mechanism of drought occurrence is complex. The synergistic effect between the two factors will significantly affect the drought conditions in the region. Attention should be paid to this in the prevention and detection of drought. In summary, these driving factors all exerted varying degrees of influence on the drought levels in the study area, with significant differences observed in their explanatory power. The main factors influencing the drought in this region are the interaction of TMP, ET and PRE with POP. Meanwhile, other factors (such as GDP and SLOPE) interact with the meteorological factors, intensifying the drought severity in the Yellow River Basin (the Henan section).

## 4 Discussion

Based on the analysis of TVDI, the results indicate that the majority of the study area was in a state of drought, with moderate drought being the dominant condition. Throughout the study period, drought conditions showed an overall trend of intensification, which is consistent with findings from previous

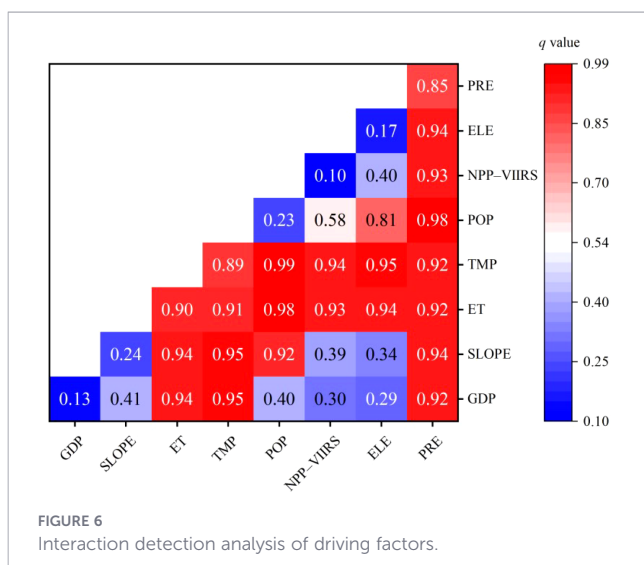
research (Zhao et al., 2022; Li Y. et al., 2024). Drought severity in the Yellow River Basin (Henan section) exhibits significant spatial heterogeneity. Specifically, the southwestern region experiences relatively lower drought intensity, with projections indicating a mitigating trend in the future. In contrast, the northeastern region suffers from higher drought severity, which is expected to intensify further under future climatic conditions. The main factors influencing drought variation are ET, TMP, and PRE. From this perspective, the drought pattern in the study area is primarily dominated by natural factors. Besides, POP interact with meteorological factors can intensify the severity of drought in this region. The considerable population size leads to substantial water requirements for agriculture, industry, and household consumption. This demand places considerable strain on water resources, thereby increasing the region's vulnerability to more severe droughts.

The utilization of water resources is closely related to land use types and methods. The land use in the southwestern region is dominated by forest land and grassland, while cultivated land is the primary in the northeastern region (Liu et al., 2025). In areas with intensive cultivated land, vegetation coverage is low, soil structure is relatively fragile, and the exposed surface area is large. Within a certain period, the soil can absorb more solar radiation, leading to increased evaporation. Furthermore, in parts of the Yellow River Basin (Henan Section) characterized by dense construction land, a large population is concentrated, thereby exacerbating the already heightened risk of drought.

Agricultural irrigation can mitigate the adverse effects of drought to some extent. However, this region faces increasingly prominent challenges, including agricultural water scarcity, an imbalance between water supply and demand, aging irrigation infrastructure, and the urgent need to transform irrigation methods. To further address the issue of agricultural drought in the study area, water conservancy projects and measurement facilities should be upgraded and modernized. Optimizing and restructuring water management agencies requires establishing a practical communication mechanism. Integrated coordination of agricultural water-saving reforms can then enhance the effectiveness of the water management system and promote greater water use efficiency (Li G. et al., 2024).

However, certain limitations were associated with the use of TVDI in studying the spatiotemporal dynamics of drought in this region. TVDI was calculated based on remote sensing data with certain time intervals, it may not fully capture rapidly evolving drought events in the region, such as sudden-onset droughts. Therefore, in terms of drought emergency monitoring and real-time decision support, there are certain limitations in using TVDI data for drought monitoring in this area.

TVDI primarily reflects surface soil moisture conditions and has limited capacity to characterize deeper soil moisture, particularly in densely vegetated mountainous areas, where it may not fully capture the actual water stress experienced by the ecosystem. It is necessary to integrate multiple indices to jointly monitor drought conditions in the Yellow River Basin (Henan section), so as to achieve a more accurate assessment of regional drought status. Furthermore, this study only conducted a zonal



analysis of drought conditions in the Yellow River Basin (Henan section) from 2003 to 2022 based on TVDI data, examining whether regional drought severity intensified or alleviated over time. While it provided a general reference for understanding drought patterns in the area, implementing specific measures to improve drought conditions in any particular zone requires more comprehensive monitoring and in-depth analysis to enable precise and targeted actions.

## 5 Conclusions

This study employed the TVDI to monitor spatiotemporal drought variations in the Yellow River Basin (Henan section). The spatial distribution and temporal trends of drought were analyzed, along with the relationships between drought and meteorological factors, topographic factors, and human activities. The following main conclusions were obtained.

1. Based on the spatial distribution of TVDI, most areas in the region were in a state of drought. Severe drought areas were concentrated in the northeastern part of Luoyang City. Only a few small areas were classified as normal regions, specifically the southwestern part of Lingbao City in Sanmenxia City, the marginal areas of Luanchuan County in Luoyang City, and the northern fringe of Jiyuan City, with TVDI values ranging from 0 to 0.46. Mild drought areas were distributed around the normal regions, with TVDI values between 0.46 and 0.57. All other areas in the region experienced moderate drought, with TVDI values ranging from 0.57 to 0.76.
2. The entire region exhibited a general increasing gradient in drought severity from the southwest to the northeast. The southwestern region experienced an alleviation of drought, reflecting an improvement in conditions. In contrast, the northeastern region witnessed a notable intensification of drought, a trend that became increasingly evident over the study period. These areas have high population density and concentrated cultivated land. Consequently, the adoption of water conservation practices and the scientific allocation of water resources are crucial for drought mitigation planning and management. Analysis using the Hurst exponent suggests that the future drought trend for the majority of the study area is expected to be opposite to that of the past. Notably, in the southwestern part of the study area, the drought situation in Sanmenxia City, Jiyuan City, and Luoning County is projected to worsen in the future. Since these are mountainous and hilly areas, the construction of water conservancy facilities and the improvement of the irrigation system will contribute to drought alleviation.
3. The main factors influencing drought conditions in the Yellow River Basin (Henan section) are ET, TMP, and PRE. Meanwhile, other factors such as POP interact with meteorological factors, which can intensify the severity of drought in this region.

## Data availability statement

The original contributions presented in the study are included in the article/supplementary material. Further inquiries can be directed to the corresponding author.

## Author contributions

ZG: Project administration, Writing – original draft, Methodology, Funding acquisition, Writing – review & editing, Conceptualization. GX: Conceptualization, Writing – review & editing, Data curation. LF: Software, Writing – review & editing, Methodology. YL: Writing – review & editing, Software. KJ: Writing – review & editing, Supervision, Formal analysis. MR: Resources, Investigation, Writing – review & editing.

## Funding

The author(s) declared that financial support was received for this work and/or its publication. This research was funded by Key Scientific and Technological Research Project of Henan Province, grant number 252102320245 and 242102320032, Key Research Projects of Higher Education Institutions in Henan Province, grant number 25A170004.

## Conflict of interest

The author(s) declared that this work was conducted in the absence of any commercial or financial relationships that could be construed as a potential conflict of interest.

## Generative AI statement

The author(s) declared that generative AI was not used in the creation of this manuscript.

Any alternative text (alt text) provided alongside figures in this article has been generated by Frontiers with the support of artificial intelligence and reasonable efforts have been made to ensure accuracy, including review by the authors wherever possible. If you identify any issues, please contact us.

## Publisher's note

All claims expressed in this article are solely those of the authors and do not necessarily represent those of their affiliated organizations, or those of the publisher, the editors and the reviewers. Any product that may be evaluated in this article, or claim that may be made by its manufacturer, is not guaranteed or endorsed by the publisher.

## References

- Abbas, H., and Ali, Z. (2024). A novel statistical framework of drought projection by improving ensemble future climate model simulations under various climate change scenarios. *Environ. Monit. Assess* 196, 938. doi: 10.1007/s10661-024-13108-w
- Alazba, A. A., Mossad, A., Geli, H. M. E., El-Shafei, A., Elkatoury, A., Ezzeldin, M., et al. (2025). Mapping land surface drought in water-scarce arid environments using satellite-based TVDI analysis. *Land* 14, 1302. doi: 10.3390/land14061302
- Ali, S., Tong, D., Xu, Z. T., Hanchiri, M., Wilson, K., Siqi, S., et al. (2019). Characterization of drought monitoring events through MODIS-and TRMM-based DSI and TVDI over South Asia during 2001–2017. *Environ. Sci. Pollut. Res.* 26, 33568–33581. doi: 10.1007/s11356-019-06500-4
- Almouctar, M. A. S., Wu, Y., Zhao, F., and Qin, C. (2024). Drought analysis using normalized difference vegetation index and land surface temperature over Niamey region, the southwestern of the Niger between 2013 and 2019. *J. Hydrol. Reg. Stud.* 52, 101689. doi: 10.1016/j.ejrh.2024.101689
- Bai, J. J., Yu, Y., and Li, P. D. (2017). Comparison between TVDI and CWSI for drought monitoring in the Guanzhong Plain, China. *J. Integr. Agric.* 16, 389–397. doi: 10.1016/S2095-3119(15)61302-8
- Bhattacharya, R. N., Gupta, V. K., and Waymire, E. (1983). The Hurst effect under trends. *J. Appl. Probab* 20, 649–662. doi: 10.1017/S0021900200023895
- Chen, T., Xia, J., Zou, L., and Hong, S. (2020). Quantifying the influences of natural factors and human activities on NVDI changes in the Hanjiang River Basin, China. *Remote Sens* 12, 3780. doi: 10.3390/rs12223780
- Chen, Z. Q., Yu, B. L., Yang, C. S., Zhou, Y. Y., Qian, X. J., Wang, C. X., et al. (2021). An extended time series, (2000–2018) of global NPP–VIIRS like nighttime light data from a cross-sensor calibration. *Earth Syst. Sci. Data* 13, 889–906. doi: 10.5194/essd-2020-201
- Chen, S., Zhang, L., Liu, X., Guo, M., and She, D. (2018). The use of SPEI and TVDI to assess temporal variations in drought conditions in the middle and lower reaches of the Yangtze River Basin, China. *Adv. Meteorol.* 1, 9362041. doi: 10.1155/2018/9362041
- Cui, M. Y., Cao, Y. P., Wang, S. K., and Yang, K. (2025). Spatiotemporal patterns and driving factors of terrestrial ecosystem gross primary productivity in the Henan Section of the Yellow River Basin. *J. Irrig. Drain* 44, 89–96. doi: 10.13522/j.cnki.ggps.2024194
- Deng, X. J., Hu, S., and Zhan, C. H. (2022). Attribution of vegetation coverage change to climate change and human activities based on the geographic detectors in the Yellow. *Environ. Sci. Pollut. Res.* 29, 44693–44708. doi: 10.1007/s11356-022-18744-8
- Fan, Y. C. (2016). The achievements and practices of soil and water conservation and ecological construction in the Yellow River Basin of Henan Province. *Soil Water Conserv. Chin.* 10, 24–26. doi: 10.14123/j.cnki.swcc.2016.0267
- Field, C., Barros, V., Stocker, T., Qin, D., Dokken, D. J., Ebi, K. L., et al. (2012). “Managing the risks of extreme events and disasters to advance climate change adaptation,” in *A special report of working groups I and II of the Inter governmental Panel on Climate Change (IPCC)* (Cambridge University Press, Cambridge, UK).
- Guo, M., Li, J., He, H. S., Xu, J. W., and Jin, Y. H. (2018). Detecting global vegetation changes using Mann–Kendall (MK) trend test for 1982–2015 time period. *Chin. Geogr. Sci.* 28, 907–919. doi: 10.1007/s11769-018-1002-2
- Guo, Q. Y., Liu, G. J., and Li, Y. X. (2020). Progress in traditional monitoring research on agricultural drought. *Rural Sci. Technol.* 20, 93–94. doi: 10.19345/j.cnki.1674-7909.2020.20.056
- Guo, E. L., Liu, X. P., Zhang, J. Q., Wang, Y. F., Wang, C. L., and Li, D. (2017). Assessing spatiotemporal variation of drought and its impact on maize yield in Northeast China. *J. Hydrol* 553, 231–247. doi: 10.1016/j.jhydrol.2017.07.060
- Huang, D., Ma, T., Liu, J., and Zhang, J. (2025). Agricultural drought monitoring using modified TVDI and dynamic drought thresholds in the upper and middle Huai River Basin, China. *J. Hydrol. Reg. Stud.* 57, 102069. doi: 10.1016/j.ejrh.2024.102069
- Hurst, H. E. (1951). Long-term storage capacity of reservoirs. *Trans. Amer. Soc. Civ. Eng.* 116, 770–808. doi: 10.1061/TACET.0006518
- Kendall, M. G. (1975). *Rank Correlation Methods* (Griffin: London, UK). doi: 10.2307/2333282
- Li, G. F., Ma, H. Y., and Zhao, C. P. (2024). The dynamic evolution and driving factors of agricultural water use efficiency in the yellow river irrigation districts: a case study of Henan province. *Chin. J. Agric. Resour. Reg. Plann* 45, 64–74. doi: 10.7621/cjarrp.1005-9121.20240907
- Li, Y., Wang, X., Wang, F., Feng, K., Li, H., Han, Y., et al. (2024). Temporal and spatial characteristics of agricultural drought based on the TVDI in Henan Province, China. *Water* 16, 1010. doi: 10.3390/w16071010
- Liu, Z. Y., and Li, J. H. (2024). Responses of temporal and spatial changes of vegetation to climate factors in Heilongjiang Province from 2000 to 2020. *For. Eng* 40, 85–97. doi: 10.3969/j.issn.1006-8023.2024.01.010
- Liu, F. Y., Ning, J., Li, S. E., He, T., Wang, A., and Su, Y. H. (2025). Ecological security pattern construction and optimization in the Yellow River Basin of Henan Province. *Ecol. Sci.* 44, 211–221. doi: 10.14108/j.cnki.1008-8873.2025.04.022
- Liu, J. M., Wang, G., Fu, X. D., Yu, S. Z., Ren, M. L., Deng, X. S., et al. (2023). Evaluation of ecological protection and high-quality development level in Henan section of the yellow river basin. *Yellow River* 45, 7–13. doi: 10.3969/j.issn.1000-1379.2023.07.002
- Mandelbrot, B. B., and Wallis, J. R. (1969). Robustness of the rescaled range R/S in the measurement of noncyclic long run statistical dependence. *Water Resour. Res.* 5, 967–988. doi: 10.1029/WR005i005p00967
- Mann, H. B. (1945). Nonparametric tests against trend. *Econometrica* 13, 245–259. doi: 10.2307/1907187
- Sandholt, I., Rasmussen, K., and Andersen, J. (2002). A simple interpretation of the surface temperature/vegetation index space for assessment of surface moisture status. *Remote Sens Environ.* 79, 213–224. doi: 10.1016/S0034-4257(01)00274-7
- Sha, Y. T., Liu, G., Zhao, X. Y., and Dong, G. H. (2024). A dataset of annual TCI, VCI, VHI and TVDI with the resolution of 1 km in the Yellow River Basin, (2003–2022). *Chin. Sci. Data* 9, 166–180. doi: 10.11922/11-6035.ncdc.2023.0006.zh
- Su, Y. Y., Lu, X. P., Xiao, F., Zhang, X. J., Li, G. Q., Yu, H. K., et al. (2024). Soil drought monitoring with TVDI and ARIMA in Henan Province. *Trans. Chin. Soc. Agric. Mach.* 55, 391–401. doi: 10.6041/j.issn.1000-1298.2024.11.038
- Wan, W., Liu, Z., Li, K., Wang, G., Wu, H., and Wang, Q. (2021). Drought monitoring of the maize planting areas in Northeast and North China Plain. *Agric. Water Manage.* 245, 106636. doi: 10.1016/j.agwat.2020.106636
- Wang, Q., Liu, Y. Y., Zhang, Y. Z., Tong, L. J., Li, X. Y., Li, J. L., et al. (2019). Assessment of spatial agglomeration of agricultural drought disaster in China from 1978 to 2016. *Sci. Rep.* 9, 14393. doi: 10.1038/s41598-019-51042-x
- Wang, J. F., and Xu, C. D. (2017). Geodetector: principle and prospective. *Acta Geogr. Sin.* 72, 116–134. doi: 10.11821/dlxb201701010
- Wang, Y. X., Yang, J., Lin, L. G., and Wei, X. D. (2023). Research on the spatio-temporal variation law of vegetation coverage in Shaanxi province based on Sen+Mann–Kendall. *Agric. Technol.* 43, 62–66. doi: 10.19754/j.nyyjs.20230415016
- Wen, Y. L., Zhou, L. W., Kang, L., Chen, H., and Guo, J. L. (2023). Drought risk analysis based on multivariate copula function in Henan Province, China. *Geomat. Nat. Hazards Risk* 14, 2223344. doi: 10.1080/19475705.2023.2223344
- Wu, C. H., Li, Z. T., Wang, S. S., and Lu, J. B. (2025). Evaluation of spatiotemporal response relationship between seasonal drought and flash drought in China from 1981 to 2021. *Water Resour. Prot.* 41, 149–157. doi: 10.3380/j.issn.1004-6933.2025.02.017
- Yan, L. J., Zhao, Y. J., Qiu, S. K., and Fu, Q. (2022). Construction and evaluation of High-quality development index system in the Yellow River Basin: take Henan section as an example. *Areal Res. Dev.* 41, 37–43. doi: 10.3969/j.issn.1003-2363.2022.06.007
- Yao, R. C., Hao, S. L., Li, X. P., Hou, J. C., Chen, H. Y., and Zhang, Y. (2024). Dynamic evolution of the vegetation and its response to climate changes from 1982 to 2020 in the Yellow River Basin (Henan section). *Geoscience* 38, 612–623. doi: 10.19657/j.geoscience.1000-8527.2024.026
- Zhao, A., Xiang, K., Zhang, A., and Zhang, X. (2022). Spatial-temporal evolution of meteorological and groundwater droughts and their relationship in the North China Plain. *J. Hydrol* 610, 127903. doi: 10.1016/j.jhydrol.2022.127903
- Zhu, Y. L., Liu, Y., Kong, X. H., Wang, X. X., Zhang, M. Q., Hong, X. W., et al. (2025). Research progress and prospect on the drought, heatwave, and compound drought and heatwave events in China. *Trans. Atmos. Sci.* 48, 26–36. doi: 10.13878/j.cnki.dqkxb.20240911002
- Zormand, S., Safari, R., and Koupaei, S. S. (2017). Assessment of PDI, MPDI and TVDI drought indices derived from MODIS Aqua/Terra Level 1B data in natural lands. *Nat. Hazards* 86, 757–777. doi: 10.1007/s11069-016-2715-0
- Zou, W., Wang, J., Li, C., Yang, K., Fetisov, D., Jiang, J., et al. (2025). Spatiotemporal analysis of drought variation from 2001 to 2023 in the China–Mongolia–Russia transboundary Heilongjiang River basin based on ITVDI. *Remote Sens.* 17, 2366. doi: 10.3390/rs17142366